

# Endostatin-induced Modulation of Plasminogen Activation with Concomitant Loss of Focal Adhesions and Actin Stress Fibers in Cultured Human Endothelial Cells<sup>1</sup>

Sara A. Wickström, Tanja Veikkola, Marko Rehn, Taina Pihlajaniemi, Kari Alitalo, and Jorma Keski-Oja<sup>2</sup>

Cell Biology and Molecular/Cancer Biology Laboratories, Biomedicum Helsinki, and Haartman Institute, Departments of Virology and Pathology, University of Helsinki, FIN-00014 Helsinki, Finland [S. A. W., T. V., K. A., J. K.-O.], and the Collagen Research Unit, Biocenter and Department of Medical Biochemistry, University of Oulu, FIN-90220 Oulu, Finland [M. R., T. P.]

## ABSTRACT

Endostatin, a  $M_r$  20,000 fragment of collagen XVIII, is able to inhibit angiogenesis and induce apoptosis in endothelial cells *in vivo*. We analyzed the effects of recombinant endostatin on human microvascular endothelial cells, focusing on pericellular plasminogen activation and its targeting by the focal adhesion-associated cytoskeletal structures. Analysis of the proteolytic plasminogen activator system revealed that endostatin modulates the distribution of soluble and cell surface-associated urokinase-type plasminogen activator (uPA) and plasminogen activator inhibitor, type 1 (PAI-1). Casein zymographic and immunoprecipitation analyses indicated that endostatin exerts its effects by decreasing the levels of soluble uPA and PAI-1 and their complexes in a dose-dependent manner. Immunofluorescence analysis of cell surface-associated uPA indicated that endostatin treatment caused the redistribution of receptor-bound uPA from focal contacts, resulting in diffuse cell surface staining. In accordance with this observation, immunofluorescence staining of the urokinase receptor revealed that endostatin treatment removed uPAR from focal adhesions. Accordingly, endostatin caused a rapid disassembly of focal adhesions as observed by immunofluorescence analysis of the focal adhesion proteins vinculin and paxillin. A prominent change in the cytoskeletal architecture was observed as the actin stress fiber network was dissociated in response to endostatin treatment. The effect of focal adhesion disassembly was reversible, persisting from 1 h up to 6 h. Our results suggest that the antiangiogenic activity of endostatin involves the modulation of focal adhesions and actin stress fibers and the down-regulation of the urokinase plasminogen activator system.

## INTRODUCTION

Angiogenesis is essential for tumor growth and survival. Hypoxic conditions in expanding tumors initiate a cascade of endothelial cell sprouting resulting in the formation of new capillary network (1). The process can be divided into distinct steps of endothelial cell activation by growth factors and cytokines and detachment and migration toward a chemotactic stimulus accompanied by degradation of the surrounding ECM<sup>3</sup> and the gradual reassembly of vessel structures (2–4). The balance between the angiogenic phenotype and endothelial cell apoptosis is governed by angiogenic growth factors, the pericellular matrix, and naturally occurring angiogenic inhibitors (3).

Antiangiogenesis is a promising field of cancer therapy, and several inhibitors of angiogenesis have been introduced (1, 5). Endostatin, the COOH-terminal  $M_r$ 20,000 fragment of collagen XVIII, is able to

inhibit angiogenesis and tumor growth in an endothelial cell-specific manner (6, 7). It is a potent inducer of endothelial cell apoptosis (8), and it is also capable of inhibiting cell proliferation and migration (7, 9); but the mechanisms behind these effects of endostatin are poorly understood thus far.

The adhesion of cells is crucial for their survival and organization. Cell adhesion is controlled by functional complexes of ECM components, transmembrane adhesion molecules, and cytoplasmic proteins (reviewed in Ref. 10). Focal adhesions represent such functional complexes, consisting of integrins, integral membrane proteoglycans, associated cytoplasmic proteins such as vinculin and paxillin, and several protein kinases. These proteins serve as anchors for actin stress fibers (11). The assembly and disassembly of the focal adhesions is a dynamic process under complex regulation as the cell converts from the adhesive to the migratory phenotype.

The uPA system comprises uPA, PAI-1, and the cell surface uPAR (12). All components of this system are constitutively expressed in endothelial cells and are up-regulated by various angiogenic growth factors, transforming growth factor- $\beta$ , and hypoxia (13–16). Through activation of plasminogen and its intrinsic proteolytic activity, uPA is able to degrade fibrin, laminin, fibronectin, proteoglycans, gelatin, and thrombospondin and activate members of other proteolytic systems and various growth factors (17). Because of its wide spectrum of proteolytic activity, uPA has been identified as an important factor in angiogenic proteolysis (18). The proteolytic activity of uPA is localized to the cell surface by glycosylphosphatidyl inositol-linked uPAR. The binding of uPA to its receptor increases the rate of plasmin formation, whereas the binding of PAI-1 to the receptor complex or soluble uPA inhibits plasminogen activation (19, 20). In addition to their role in targeted proteolysis, uPA, PAI-1, and uPAR play a role in cell adhesion and migration (21–24). Proteolytic activity dependent on uPA localizes at the leading edge of migrating endothelial cells forming tubular structures and, more specifically, to focal adhesions (25).

We report here that endostatin interferes with the targeting of pericellular proteolysis by down-regulating the levels of secreted soluble uPA and PAI-1 and their complexes and by removing uPAR-associated uPA from the focal adhesions. This is accompanied by the disassembly of focal adhesion complexes and the reassembly of the actin cytoskeleton by disruption of stress fibers in response to endostatin treatment. These changes plausibly affect the adhesive, migratory, and apoptotic behavior of endothelial cells.

## MATERIALS AND METHODS

**Reagents and Antibodies.** Human plasminogen was from Chromogenix (Mölnådal, Sweden), and high molecular weight-uPA was from Calbiochem (San Diego, CA). Mouse monoclonal antibodies against paxillin were from Signal Transduction Laboratories (Lexington, KY). Rabbit polyclonal anti-uPA and murine monoclonal anti-PAI-1 were from American Diagnostica, Inc. (Greenwich, CT). Mouse monoclonal anti-vinculin antibody was from Sigma Chemical Co. (St. Louis, MO). mAB R4 (26) against uPAR was a gift from Dr. Keld Danø (Finsen Laboratory, Denmark).

**Cell Culture.** HDMECs were purchased from Promocell (Heidelberg, Germany) and were cultured in Endothelial Cell Growth Medium (Promocell) at

Received 10/30/00; accepted 7/3/01.

The costs of publication of this article were defrayed in part by the payment of page charges. This article must therefore be hereby marked *advertisement* in accordance with 18 U.S.C. Section 1734 solely to indicate this fact.

<sup>1</sup> This work was supported by the Academy of Finland, the Sigrid Juselius Foundation, Biocentrum Helsinki, the Helsinki University Hospital Fund, the Novo Nordisk Foundation, the Finnish Cancer Foundation, the Emil Aaltonen Foundation, the Farnos Research and Science Foundation, and the University of Helsinki.

<sup>2</sup> To whom requests for reprints should be addressed, at Biomedicum Helsinki, Laboratory of Cell Biology, PL 63 (Haartmaninkatu 8), FIN-00014, University of Helsinki, Finland. Phone: 358-9-191-25566; Fax: 358-9-191-25573; Email: Jorma.Keski-Oja@Helsinki.fi.

<sup>3</sup> The abbreviations used are: ECM, extracellular matrix; uPA, urokinase-type plasminogen activator; PAI-1, plasminogen activator inhibitor, type 1; uPAR, urokinase-type plasminogen activator receptor; HDMEC, human dermal microvascular endothelial cell; mAB, monoclonal antibody; TRITC, rhodamine isothiocyanate; PA, plasminogen activator; MMP, matrix metalloproteinase.

37°C in a humidified 5% CO<sub>2</sub> atmosphere. The cells used for the experiments between were undergoing passages 3–6. Human embryonic lung fibroblasts (CCL-137; American Type Culture Collection, Rockville, MD) were cultured in Eagle's minimal essential medium supplemented with 10% FCS, 100 IU ml<sup>-1</sup> of penicillin, and 50 µg ml<sup>-1</sup> of streptomycin. The cells were washed twice with serum-free medium and incubated for at least 6 h before treatment with the various chemicals. All experiments were carried out under serum-free conditions.

**Expression and Characterization of Recombinant Human Endostatin.** Recombinant human endostatin was expressed and purified as described (27). A fragment of human collagen XVIII that corresponds to mouse endostatin sequences (6) was cloned to the vector pQE-31 (Qiagen, Santa Clarita, CA) and expressed as an NH<sub>2</sub>-terminal His-tagged protein in *Escherichia coli* strain M15, according to the manufacturer's protocol (Qiagen). Bacterial pellets were lysed in 6 M guanidine HCl, 0.5 M NaCl, 10 mM β-mercaptoethanol, and 20 mM Tris-HCl (pH 7.9) by freeze-thaw and then centrifuged. The supernatant was lightly sonicated and applied to a ProBond column (Invitrogen, San Diego, CA) that had been preequilibrated with 8 M urea, 0.5 M NaCl, and 20 mM Tris-HCl (pH 7.9). Bound protein was eluted by an imidazole gradient from 0 to 0.5 M in the equilibrium buffer. Endostatin fractions were pooled and refolded *in vitro*, first by dialyzing overnight at 4°C against 4 M urea, 0.1 M NaCl, 1 mM/0.1 mM reduced/oxidized glutathione, and 20 mM Tris-HCl (pH 7.9), then dialyzed for 6 h against 1 M urea, 0.1 M NaCl, 0.1 mM/0.01 mM reduced/oxidized glutathione, 20 mM Tris-HCl (pH 7.9), and finally dialyzed overnight against PBS [170 mM NaCl and 10 mM sodium phosphate buffer (pH 6.9)]. Refolded soluble endostatin was separated by centrifugation and applied to a HiTrap SP cation-exchange column (Amersham Pharmacia, Piscataway, NJ). Endostatin fractions were eluted by a NaCl gradient from 0.1 M to 1.5 M in PBS (pH 6.9), pooled and dialyzed against 0.1 M NaCl and 20 mM Tris-HCl (pH 7.4), and applied to a heparin-Sepharose CL-6B column (Amersham Pharmacia, Piscataway, NJ). Bound endostatin was eluted by a NaCl gradient from 0.1 M to 2 M in 20 mM Tris-HCl (pH 7.4). Endostatin fractions were pooled and dialyzed against PBS (pH 7.4) and passed through a Polymyxin agarose column using PBS buffer. Purified endostatin was concentrated by ultrafiltration to 0.5–1.5 mg/ml and stored at -20°C until use. Far UV circular dichroism spectrum was recorded on an AVIV Associates (Lakewood, NJ) model 62DS spectrometer. Buffer conditions in the circular dichroism analysis were 10 mM potassium phosphate (pH 8.0), and cells of 1 mm path length were used. A 5-s time constant and a 1.0 nm bandwidth was used during data acquisition over a wavelength range of 184 to 260 nm; three spectra were collected for protein or buffer and were averaged. Buffer spectra were subtracted from the protein spectra. No endotoxin was found in the purified fractions. The biological activity of endostatin was confirmed in a three-dimensional collagen tube formation assay where endostatin effectively inhibited growth factor-induced endothelial cell tube formation (data not shown). The concentrations used in this study are in agreement with amounts used commonly in cell culture, and possible differences can be explained by the different sources of endostatin (9).

**Casein Zymography.** Zymography and reverse zymography were used to identify the molecular forms of uPA and PAI (28). Polypeptides of conditioned media or acid eluates were separated under nonreducing conditions in gradient polyacrylamide gels (4–15%) in the presence of SDS (Bio-Rad, Hercules, CA). SDS was removed by washing the gels with PBS (pH 7.4)/Triton X-100 (2.5%) 4 × 15 min. For reverse zymography, reducing conditions were used, and uPA (2 IU/ml) was added to the final wash. The gels were then placed on caseinolysis gels containing plasminogen and casein in 1.2% agarose and incubated at 37°C until the lytic bands correlating to the PA-activity became visible. A lysis resistant band indicated the migration of PAI.

**Analysis of Membrane-bound PA Activity.** Analysis of membrane-bound PA activity was performed essentially as described (29). Endothelial cells were washed with 0.2% BSA in PBS (pH 7.4) and treated with 50 mM glycine-HCl buffer (pH 3.0), containing 0.1 M NaCl at room temperature for 10 min. The buffer was collected, immediately neutralized, and subjected to casein zymography.

To test whether the cell surface accumulation could be prevented by blocking uPAR, blocking mAbs against uPAR were added to cells at a concentration of 30 µg/ml before the addition of 40 nM endostatin. Mouse IgG was used as a negative control. The treatment was carried out for 4 h, after which the cell surface proteins were collected with acid elution, as described

above. The eluates were subsequently subjected to casein zymography to reveal the eluted PAs.

**Metabolic Labeling and Immunoprecipitation.** Serum-starved cells were incubated with endostatin for 4 h in [<sup>35</sup>S]methionine (80 µCi/ml; Amersham Pharmacia Biotech, Uppsala, Sweden) in methionine-free medium. Subsequently, aliquots of conditioned media were subjected to immunoprecipitation. Samples were preabsorbed by incubation with mouse preimmune serum and protein A-Sepharose beads at 4°C in an end-over mixer for 2 h. The beads were removed by centrifugation and the supernatants were incubated with antibodies against uPA or PAI-1 on ice for 30 min. γ-bind Sepharose (Amersham Pharmacia, Uppsala, Sweden) was added, and the samples were incubated in an end-over mixer at 4°C for 1 h. The beads were subsequently collected by centrifugation and washed three times with Triton lysis buffer [50 mM Tris-HCl buffer (pH 8.0) containing 150 mM NaCl, 1% Triton X-100, 0.02% sodium azide, 10 mM EDTA, 10 µg/ml aprotinin, 1 µg/ml pepstatin A, and 1 µg/ml aminoethylbenzene sulfonyl fluoride; Calbiochem, San Diego, CA). The bound proteins were eluted with Laemmli sample buffer. The eluted polypeptides were separated by 4–15% gradient PAGE in the presence of SDS under nonreducing conditions and visualized by autoradiography. Incorporated radioactivity was detected and quantitated with the Fuji film BAS-2500 Image Analyzer and the MacBAS 2.5 computer program. The quantified radioactive intensities were normalized with the background intensities of each lane to account for possible differences in sample loading.

**Immunofluorescence.** The cells were cultured on glass coverslips and allowed to grow until subconfluency. After the treatments, the cells were washed with PBS and fixed with 3% paraformaldehyde at 4°C for 10 min. The cells were then treated with 5% BSA for 30 min, washed with PBS (pH 7.4), and incubated with polyclonal antibodies against uPA or with monoclonal antibodies against vinculin or paxillin. TRITC-conjugated phalloidin (Sigma Chemical Co.) was used for the staining of the actin cytoskeleton. Unbound proteins were removed by washing with subsequent incubation with Cy3- or FITC-labeled secondary antibodies (Jackson ImmunoResearch Laboratories, West Grove, PA), respectively, for 1 h. For the immunolocalization of uPAR, cells were cultured on glass coverslips and treated with endostatin and then washed with cold PBS (pH 7.4). Cells were then incubated with antibodies against uPAR at 4°C for 20 min, washed with PBS, and fixed with 3% paraformaldehyde. Subsequently, the cells were washed with PBS and incubated with Cy3-labeled secondary antibodies for 1 h. The coverslips were then washed and mounted on glass slides using Vectashield (Vector Laboratories, Burlingame, CA). The fluorescent images were obtained using an epifluorescent microscope.

## RESULTS

### Effects of Endostatin on the Levels of Soluble uPA and PAI-1.

To analyze the effects of endostatin on the PA system, we studied the levels of secreted uPA and PAI-1 in cultures of human microvascular endothelial cells. The cells were incubated with increasing concentrations of endostatin, and aliquots of the conditioned media were collected at the indicated time points and subjected to casein zymography. The uPA seemed mostly in a complex with its inhibitor PAI-1 in this assay, but the latter is inactivated by SDS treatment. uPA is therefore reactivated and visualized as a lysis zone. We found that endostatin decreased the levels of uPA/PAI-1 complexes secreted into the culture medium in a concentration-dependent manner within 8 h (Fig. 1A). The differences in uPA/PAI-1 levels became visible at 6 h, reaching a maximum within 12 h (Fig. 1B).

To independently assess the levels of secreted PAI-1, the cells were treated with endostatin as described above, and aliquots of the media were subjected to reverse zymography. Inspection of the reverse zymograms indicated that the levels of secreted PAI-1 decreased proportionally in response to increasing concentrations of endostatin during 8 h of incubation (Fig. 1A). The effect of endostatin reached a maximum in 12 h (Fig. 1B). No change in the caseinolytic activity was observed when endostatin was added to the media aliquots after their collection or when incubated on caseinolysis gels together with puri-

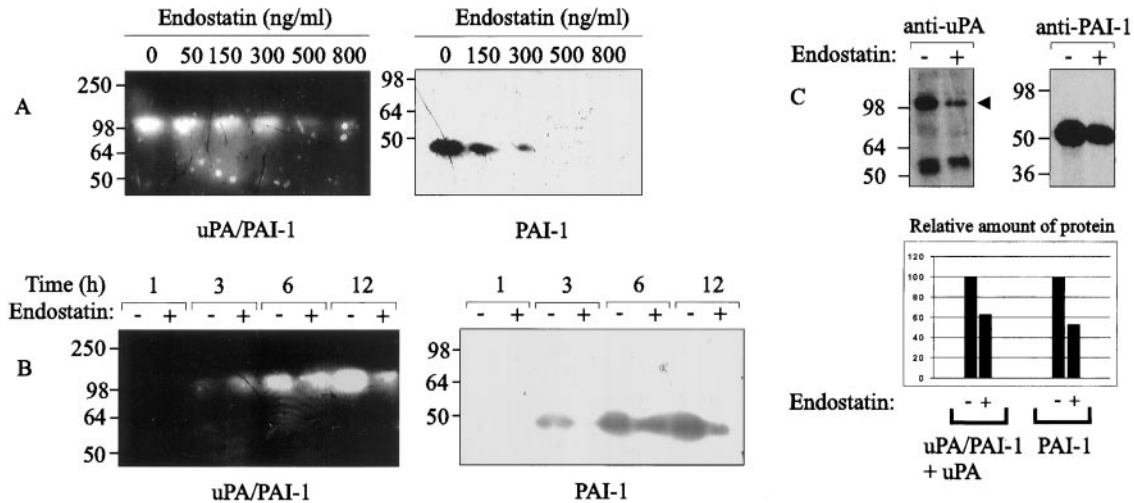


Fig. 1. Endostatin down-regulates the levels of soluble secreted uPA and PAI-1. *A*, dose-dependency analysis. Cells were incubated with increasing concentrations of endostatin for 8 h before the collection of the media. Aliquots of the conditioned media were then subjected to casein zymography under nonreducing (for zymography) or reducing (for reverse zymography) conditions. The zymogram (*left*) reveals a single lytic band of  $M_r \sim 98,000$ , corresponding to the uPA/PAI-1 complex. Reverse zymography (*right*) shows lysis-resistant bands representing PAI-1. Note the dose-dependent decrease of both uPA/PAI-1 complexes and PAI-1 in endostatin-treated cultures. *B*, time-dependency analysis. Cells were treated with endostatin (40 nM; 800 ng/ml), and aliquots of the conditioned media were collected after the indicated incubation periods, with subsequent zymography (uPA/PAI-1) and reverse zymography for PAI-1. *C*, immunoprecipitation analysis. Cells were labeled with [ $^{35}$ S]methionine during incubation with 40 nM endostatin (800 ng/ml) for 4 h. The radiolabeled proteins from the conditioned media were then immunoprecipitated using antibodies against uPA or PAI-1, separated by 4–15% gradient PAGE in the presence of SDS, and visualized by autoradiography. The migration of molecular weight markers (kDa) is shown on the *left*. *Arrowhead*, migration of the uPA/PAI-1 complex. *Graph* below the autoradiograph illustrates the incorporated radioactivities corresponding to precipitated uPA and PAI-1. The bands were quantitated by Phospho-Imager analysis and plotted as relative protein levels. The quantitative analysis revealed that the levels of uPA and PAI-1 were about 60 and 50% lower, respectively, in endostatin-treated cells than in control cells.

fied human uPA, indicating that endostatin itself does not affect uPA activity (data not shown).

To confirm the results obtained by zymography, HDMECs were metabolically labeled with [ $^{35}$ S]methionine for 4 h in the presence of endostatin as described in “Materials and Methods.” Conditioned medium was then collected and subjected to immunoprecipitation with anti-uPA and anti-PAI-1 antibodies (Fig. 1C). Quantitation of the incorporated radioactivity of the precipitated bands indicated that the levels of secreted uPA and PAI were lower in the endostatin-treated cells than in the control cells (Fig. 1C). Aliquots of conditioned media of endostatin treated cells were then subjected to ELISA-analysis. A similar but slightly less prominent down-regulation of uPA and PAI-1 after endostatin-treatment was observed in this assay.<sup>4</sup>

To assess whether the decrease observed in uPA and PAI-1 levels was caused by transcriptional regulation, Northern blotting analysis was performed on endostatin-treated cells. No changes in the mRNA levels of uPA or PAI-1 were observed within 6–12 h of endostatin treatment (data not shown).

**Redistribution of Cell Surface-associated uPA and uPAR by Endostatin.** The localization of proteolytic activity to distinct compartments of the cell surface is crucial for the effective degradation of the surrounding matrix (12, 30). PA activity is localized to focal adhesions through its cell surface receptor uPAR. To analyze the effect of endostatin on the cell surface localization of uPA, the cells were treated with endostatin for 3 h and fixed with 3% paraformaldehyde. The fixed cells were stained with specific antibodies against uPA. Control cells showed a distinct localization of uPA in focal adhesions, which was confirmed with double staining for vinculin. Endostatin-treated cells, on the other hand, exhibited a diffuse staining pattern. The effect appeared in parallel with the loss of vinculin staining from the focal adhesions at 1 h, but no relocalization of uPA into the recovered focal adhesions was observed within 6 h of treatment (Fig. 2A). Cells incubated with phosphoinositol-specific phospholipase-C (Sigma Chemical Co.) before immunostaining showed no

positive staining with antibodies against uPA, confirming the specificity of the staining for uPA-occupied uPAR.

To analyze whether the redistribution of uPA was associated with changes in the cell surface localization of uPAR, monoclonal antibodies were used to immunostain uPAR in endostatin-treated cells. Control cells displayed a staining pattern closely resembling that of uPA, where positive staining was observed mostly in focal adhesion plaques. This pattern was strongly disrupted by treatment with 40 nM endostatin, resulting in diffuse cell surface staining of uPAR within 1 h of incubation (Fig. 2B).

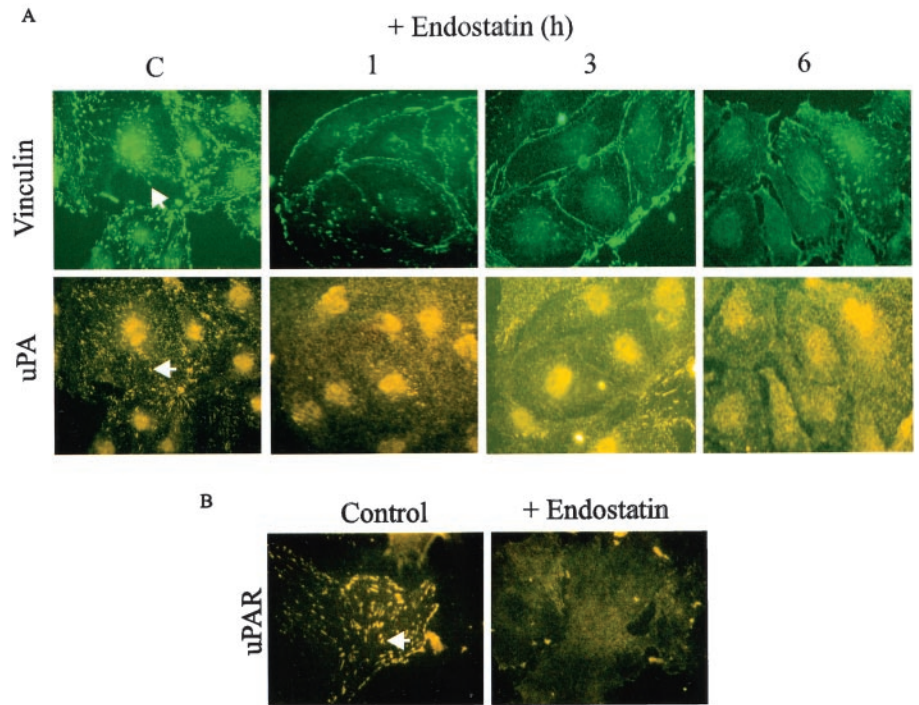
To investigate the observation further, we carried out experiments where endothelial cells were incubated with increasing concentrations of endostatin. After 3 h of incubation, the cell surface-associated proteins were eluted with a mild acid treatment and analyzed with casein zymography. These experiments revealed that endostatin increased the amounts of uPA/PAI-1 complexes at the cell surface in a dose-dependent manner, as detected by acid elution (Fig. 3A). Only negligible levels of free uPA were detected under these conditions.

Next, we sought to investigate whether the cell surface accumulation of uPA/PAI-1 complexes was dependent on the cell surface receptor, uPAR. Blocking mAbs against uPAR were added to cells before the administration of 40 nM endostatin. Mouse IgG was added to the control cells. After 3 h of incubation, the cell surface proteins were collected by acid elution and analyzed with casein zymography. Inspection of the zymographs revealed that blocking of uPAR by the mAb inhibits the cell surface accumulation of uPA/PAI-1 complexes. This is seen both in endostatin-treated and control cells. In addition, blocking of uPAR by mAbs inhibits the up-regulation of uPA/PAI-1 complexes at the cell surface by endostatin treatment (Fig. 3B).

**Disruption of Focal Adhesions and the Actin Stress Fibers by Endostatin.** The redistribution of uPA and vinculin suggested that endostatin has an effect on focal adhesions, which are functional complexes involved in cell adhesion and in migration on the pericellular matrix (11). HDMECs grown on glass coverslips displayed prominent focal adhesions, as visualized both by anti-vinculin and anti-paxillin immunofluorescent staining. The focal adhesions ap-

<sup>4</sup> S. Wickström, T. Veikkola, K. Alitalo, and J. Keski-Oja, unpublished observations.

Fig. 2. Endostatin treatment induces loss of uPA from the focal contacts. *A*, subconfluent cultures of endothelial cells were treated with 40 nM endostatin (800 ng/ml) for 1–6 h, as indicated on the figure, and immunostained with antibodies against vinculin or uPA. *Arrowheads*, intact focal adhesions. Note the disassembly of vinculin-stained focal adhesions after 1 h of endostatin treatment accompanied by the dissociation of uPA from these structures. Evidence for focal adhesion recovery (vinculin staining) was seen after 6 h, but uPA remained diffusely redistributed at the cell surface. *C*, untreated control cells. *B*, HDMECs were treated with 40 nM endostatin for 1 h and immunostained with antibodies against uPAR. Note the localization of uPAR in focal adhesion plaques in control cells, indicated by *arrowheads*, and the diffuse staining pattern in endostatin-treated cells.



peared characteristically as short streaks in the basal surface of the cytoplasm. Treatment of spread cells with 40 nM endostatin (800 ng/ml) for 1 h caused a dramatic reduction in the number of cells containing such a staining pattern. The endostatin-treated cells dis-

played vinculin staining restricted to cell-cell junctions and weak paxillin staining distributed diffusely throughout the cytoplasm. The majority of the cells were devoid of the cytoplasmic streaks (Fig. 4A). The disruption of focal adhesions had occurred already after 1 h of treatment and persisted for at least 3 h of incubation, whereas evidence of focal adhesion recovery was observed after 6 h of incubation (Fig. 2).

The cellular actin stress fibers, which form a major part of the cytoskeleton, are known to terminate in the focal adhesion complexes. The effect of endostatin on the organization of the actin cytoskeleton was assessed next. The cells were grown to subconfluency, treated with endostatin for 1 h, and stained for actin using TRITC-conjugated phalloidin. Control cells showed staining of actin stress fibers traversing the cytoplasm plus a layer of cortical actin. Endostatin-treated cells stained less intensely with TRITC-phalloidin, and the stress fiber network was largely disorganized; however, the cortical actin bundles remained intact (Fig. 4A). Previously it has been observed that the effects of endostatin are endothelial cell-specific (6). To determine whether the endostatin-induced alterations of the cytoskeletal structure are limited to endothelial cells, human embryonic lung fibroblasts were treated with 40 nM endostatin for 1 h. No changes in the distribution of focal adhesions were observed in cells stained with antibodies against vinculin or paxillin. Accordingly, no changes in the distribution of actin were observed with TRITC-phalloidin staining (Fig. 4B).

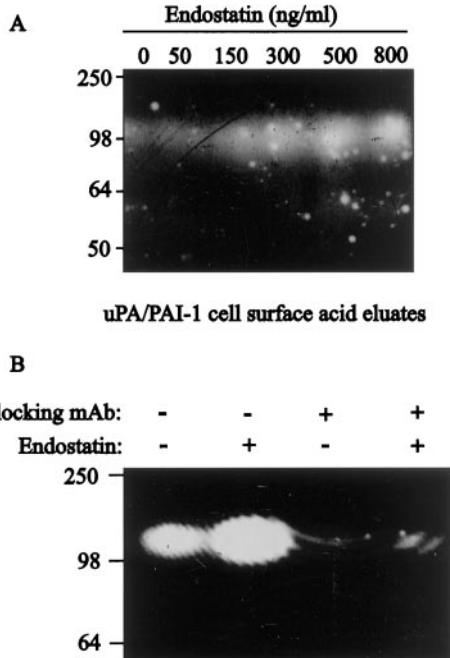
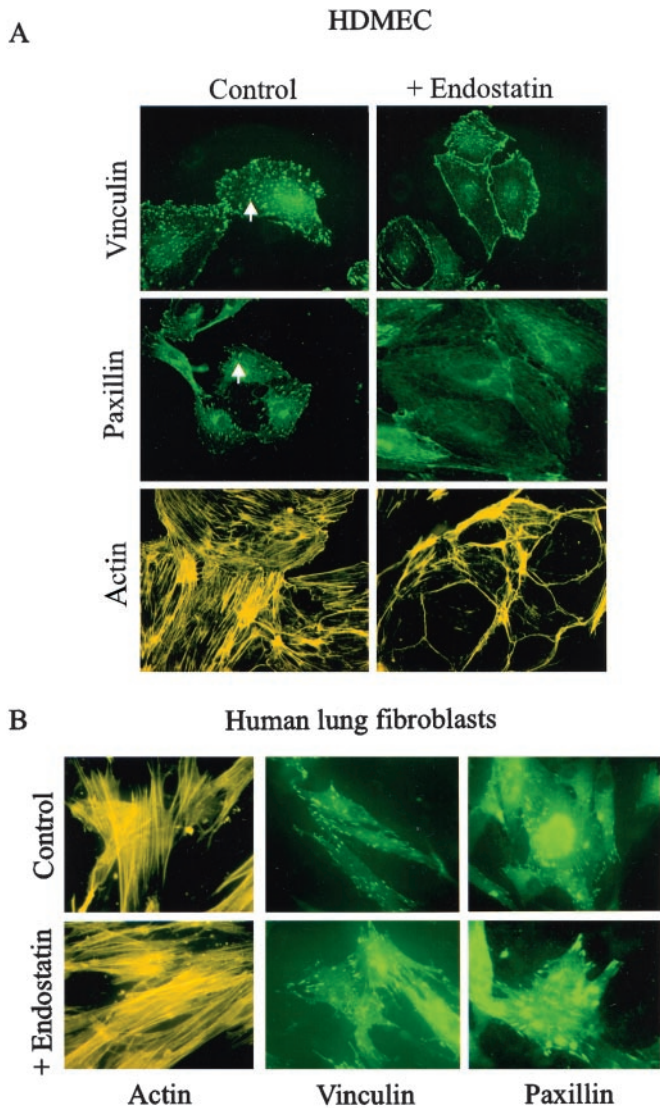


Fig. 3. Effects of endostatin on cell surface-associated uPA/PAI-1 complexes. *A*, endothelial cells were grown to confluency and treated with increasing concentrations of endostatin for 4 h. Cell surface-associated protein complexes were then isolated by mild acid treatment for 5 min and subjected to casein zymography. Note the dose-dependent increase in the caseinolytic activity of the cell-layer associated uPA/PAI-1-complexes. *B*, confluent HDMECs were treated with 40 nM endostatin together with a blocking mAb against uPAR. Control cells were incubated with mouse IgG. Cell surface-associated protein complexes were then isolated by a mild acid treatment for 5 min and subjected to casein zymography. Note that the blocking mAbs against uPAR inhibit the cell surface accumulation of uPA/PAI-1 complexes and abolish the endostatin-induced increase in cell surface-associated uPA/PAI-1.

DISCUSSION

We analyzed the effects of the angiogenesis inhibitor endostatin on human endothelial cell surface PA levels. On the basis of the dramatic effects of endostatin on uPA localization, we carried out an analysis of the cytoskeletal structure. First we discovered that endostatin effectively modulates components of the PA system, and subsequently we found that also the cytoskeletal structures known to be involved in endothelial cell migration and matrix invasion were affected. As a response to endostatin treatment, pericellular proteolytic activity was redistributed and down-regulated as monitored by analysis of uroki-



**Fig. 4.** Redistribution of focal adhesion proteins and actin by endostatin treatment. **A**, HDMECs were grown on glass coverslips until subconfluency and treated with 40 nM endostatin for 1 h. The cells were fixed with 3% paraformaldehyde and immunostained with antibodies against vinculin or paxillin, or with TRITC-conjugated phalloidin, as indicated. *Arrowheads*, intact focal adhesions. Note that endostatin-treated cells lack vinculin- and paxillin-staining of cytoplasmic focal adhesions as well as the prominent actin stress fiber network visualized by TRITC-phalloidin staining. **B**, CCL-137 human lung fibroblasts grown on glass coverslips were treated with 40 nM endostatin for 1 h, fixed, and immunostained with antibodies against vinculin or paxillin, or with TRITC-phalloidin, as indicated. Note that neither the prominent focal adhesion plaques nor the actin fiber network were affected by endostatin in fibroblastic cells.

nase PA activity. These changes were accompanied by rapid disassembly of focal adhesion proteins paxillin and vinculin, and reorganization of the actin cytoskeleton

Proteolytic activity is a prerequisite for endothelial cell sprouting and tube formation (4, 31). Culturing endothelial cells in type I collagen or stimulation with angiogenic growth factors such as basic fibroblast growth factor have been observed to increase the secretion of both uPA and PAI-1 (32). For efficient proteolysis, proteases are targeted to distinct locations at the cell surface and, in particular, changes in uPA and PAI-1 secretion and localization can induce changes in cell migration and adhesion (33–35). Our current results indicate that endostatin modulates both the amount and the localization of uPA and PAI-1 in endothelial cell cultures. We found that the levels of uPA and PAI-1 were decreased in the conditioned media of endothelial cells after endostatin treatment. Whether the observed

down-regulation of secreted proteolytic activity is an independent phenomenon or a consequence of focal and cytoskeletal reorganization is not known yet (see Ref. 36).

Microvascular endothelial cells stained with antibodies against uPA and uPAR showed a strong signal in focal adhesions, whereas the cells treated with endostatin displayed a diffuse staining pattern. At the same time, the uPA/PAI-1 complexes isolated from the cell surface by acid treatment were increased in a dose-dependent manner. However, no significant increase in the levels of uPA or PAI-1 was detected in the immunoprecipitates of cell lysates or ECM preparations after the metabolic labeling of endostatin-treated cells, indicating that the increase of cell surface uPA/PAI-1 complexes is not attributable to intracellular or matrix accumulation of these proteins. The finding that up-regulation of acid-eluted uPA/PAI-1 complexes could be inhibited by blocking the cell surface receptor uPAR further elucidates this effect. The relocation of uPA and uPAR may be a consequence of the focal adhesion disassembly.

Interestingly, the regulation of plasminogen activation is modulated by another antiangiogenic molecule, angiostatin, which has displayed a synergistic effect with endostatin (37, 38). Another important family of proteinases, the MMPs, has also been assessed by us as a possible target for endostatin. No changes in gelatinase A (MMP-2) activation were detected by gelatin zymography assays of conditioned media in response to endostatin treatment. The proteolytic processing of membrane-type-1 MMP and its localization on the cell surface, phenomena linked with efficient proteolysis (39), were also unaffected.<sup>4</sup>

Cell migration in angiogenesis involves concerted assembly and disassembly of focal adhesions in the polarized endothelial cells. The process is thought to require parallel signaling through integrins and transmembrane proteoglycans (40), both putative binding sites for endostatin (41, 27). Our results indicate that endostatin interferes with this system by disassembling focal adhesions as visualized by immunofluorescence staining with antibodies against two major components of the adhesion complex, vinculin and paxillin. The effect was rapid, already visible 1 h after endostatin administration, and persisted for up to 6 h. The reversibility of the observation suggests the cytoskeletal changes to be an independent phenomenon rather than a sign of apoptotic behavior.

Changes in cell-substratum interactions in adherent and motile cells are transduced through the focal adhesions into the actin cytoskeleton, which is responsible for the mechanical forces generated within the cell. Intact focal adhesions are required for actin stress fiber formation and anchorage. We observed that endostatin induced a marked rearrangement of the endothelial actin network, because the stress fibers were no longer detectable in contrast with their well-organized pattern of in control cells. This finding supports the view that the absence of paxillin and vinculin staining in focal adhesions is caused by the disassembly of the entire complexes rather than by failure to recruit these proteins to existing adhesion structures. The cellular mechanisms behind these changes remain unclear at present. It should be noted that endostatin affects cell survival, proliferation, and migration (7, 8, 9), all events controlled in part by cell-substratum interactions. Interference with focal adhesion and actin cytoskeleton assembly as well as targeted proteolysis provide plausible mechanisms for these effects.

**ACKNOWLEDGMENTS**

We thank Sami Starast for fine technical assistance.

**REFERENCES**

1. Folkman, J. Angiogenesis in cancer, vascular, rheumatoid and other disease. *Nat. Med.*, 1: 27–31, 1995.

2. Klagsbrun, M., and D'Amore, P. A. Regulators of angiogenesis. *Annu. Rev. Physiol.*, *53*: 217–239, 1991.
3. Hanahan, D., and Folkman, J. Patterns and emerging mechanisms of the angiogenic switch during tumorigenesis. *Cell*, *86*: 353–364, 1996.
4. Risau, W. Mechanisms of angiogenesis. *Nature (Lond.)*, *386*: 671–674, 1997.
5. Bergers, G., Javaherian, K., Lo, K. M., Folkman, J., and Hanahan, D. Effects of angiogenesis inhibitors on multistage carcinogenesis in mice. *Science (Wash. DC)*, *284*: 808–812, 1999.
6. O'Reilly, M. S., Boehm, T., Shing, Y., Fukai, N., Vasios, G., Lane, W. S., Flynn, E., Birkhead, J. R., Olsen, B. R., and Folkman, J. Endostatin: an endogenous inhibitor of angiogenesis and tumor growth. *Cell*, *88*: 277–285, 1997.
7. Dhanabal, M., Volk, R., Ramchandran, R., Simons, M., and Sukhatme, V. P. Cloning, expression, and *in vitro* activity of human endostatin. *Biochem. Biophys. Res. Commun.*, *258*: 345–352, 1999.
8. Dhanabal, M., Ramchandran, R., Waterman, M. J. F., Lu, H., Knebelmann, B., Segal, M., and Sukhatme, V. P. Endostatin induces endothelial cell apoptosis. *J. Biol. Chem.*, *274*: 11721–11726, 1999.
9. Yamaguchi, N., Anand-Apte, B., Lee, M., Sasaki, T., Fukai, N., Shapiro, R., Que, I., Lowik, C., Timpl, R., and Olsen, B. R. Endostatin inhibits VEGF-induced endothelial cell migration and tumor growth independently of zinc binding. *EMBO J.*, *18*: 4414–4423, 1999.
10. Gumbiner, B. M. Cell adhesion: the molecular basis of tissue architecture and morphogenesis. *Cell*, *84*: 345–357, 1996.
11. Jockusch, B. M., Bubeck, P., Giehl, K., Kroemker, M., Moschner, J., Rothkegel, M., Rudiger, M., Schluter, K., Stanke, G., and Winkler, J. The molecular architecture of focal adhesions. *Annu. Rev. Cell Dev. Biol.*, *11*: 379–416, 1995.
12. Danø, K., Romer, J., Nielsen, B. S., Bjorn, S., Pyke, C., Rygaard, J., and Lund, L. R. Cancer invasion and tissue remodeling—cooperation of protease systems and cell types. *APMIS*, *107*: 120–127, 1999.
13. Laiho, M., Saksela, O., Andreasen, P. A., and Keski-Oja, J. Enhanced production and extracellular deposition of the endothelial-type plasminogen activator inhibitor in cultured human lung fibroblasts by transforming growth factor- $\beta$ . *J. Cell Biol.*, *103*: 2403–2410, 1986.
14. Laiho, M., and Keski-Oja, J. Growth factors in the regulation of pericellular proteolysis: a review. *Cancer Res.*, *49*: 2533–2553, 1989.
15. Pinsky, D. J., Liao, H., Lawson, C. A., Yan, S. F., Chen, J., Carmeliet, P., Loskutoff, D. J., and Stern, D. M. Coordinated induction of plasminogen activator inhibitor-1 (PAI-1) and inhibition of plasminogen activator gene expression by hypoxia promotes pulmonary vascular fibrin deposition. *J. Clin. Invest.*, *102*: 919–928, 1998.
16. Graham, C. H., Fitzpatrick, T. E., and McCrae, K. R. Hypoxia stimulates urokinase receptor expression through a heme protein-dependent pathway. *Blood*, *91*: 3300–3307, 1998.
17. Kwaan, H. C. The plasminogen-plasmin system in malignancy. *Cancer Metast. Rev.*, *11*: 291–311, 1992.
18. Schnaper, H. W., Barnathan, E. S., Mazar, A., Maheshwari, S., Ellis, S., Cortez, S. L., Baricos, W. H., and Kleinman, H. K. Plasminogen activators augment endothelial cell organization *in vitro* by two distinct pathways. *J. Cell. Physiol.*, *165*: 107–118, 1995.
19. Behrendt, N., Rønne, E., and Danø, K. The structure and function of the urokinase receptor, a membrane protein governing plasminogen activation on the cell surface. *Biol. Chem. Hoppe Seyler*, *376*: 269–279, 1995.
20. Ellis, V., Wun, T. C., Behrendt, N., Ronne, E., and Danø, K. Inhibition of receptor-bound urokinase by plasminogen-activator inhibitors. *J. Biol. Chem.*, *265*: 9904–9908, 1990.
21. Wei, Y., Waltz, D. A., Rao, N., Drummond, R. J., Rosenberg, S., and Chapman, H. A. Identification of the urokinase receptor as an adhesion receptor for vitronectin. *J. Biol. Chem.*, *269*: 32380–32388, 1994.
22. Busso, N., Masur, S. K., Lazega, D., Waxman, S., and Ossowski, L. Induction of cell migration by pro-urokinase binding to its receptor: possible mechanism for signal transduction in human epithelial cells. *J. Cell Biol.*, *126*: 259–270, 1994.
23. Kanse, S. M., Kost, C., Wilhelm, O. G., Andreasen, P. A., and Preissner, K. T. The urokinase receptor is a major vitronectin-binding protein on endothelial cells. *Exp. Cell Res.*, *224*: 344–353, 1996.
24. Stefansson, S., and Lawrence, D. A. The serpin PAI-1 inhibits cell migration by blocking integrin  $\alpha$  V  $\beta$  3 binding to vitronectin. *Nature (Lond.)*, *383*: 441–443, 1996.
25. Kroon, M. E., Koolwijk, P., van Goor, H., Weidle, U. H., Collen, A., van der Pluijm, G., and van Hinsbergh, V. W. Role and localization of urokinase receptor in the formation of new microvascular structures in fibrin matrices. *Am. J. Pathol.*, *154*: 1731–1742, 1999.
26. Rønne, E., Behrendt, N., Ellis, V., Ploug, M., Danø, K., and Høyer-Hansen, G. Cell-induced potentiation of the plasminogen activation system is abolished by a monoclonal antibody that recognizes the NH<sub>2</sub>-terminal domain of the urokinase receptor. *FEBS Lett.*, *288*: 233–236, 1991.
27. Rehn, M., Veikkola, T., Kukk-Valdre, E., Nakamura, H., Ilmonen, M., Lombardo, C., Pihlajaniemi, T., Alitalo, K., and Vuori, K. Interaction of endostatin with integrins implicated in angiogenesis. *Proc. Natl. Acad. Sci.*, *98*: 1024–1029, 2001.
28. Granelli-Piperno, A., and Reich, E. A study of proteases and protease-inhibitor complexes in biological fluids. *J. Exp. Med.*, *148*: 223–234, 1978.
29. Stoppelli, M. P., Tacchetti, C., Cubellis, M. V., Corti, A., Hearing, V. J., Cassani, G., Appella, E., and Blasi, F. Autocrine saturation of pro-urokinase receptors on human A431 cells. *Cell*, *45*: 675–684, 1986.
30. Mignatti, P., and Rifkin, D. B. Nonenzymatic interactions between proteinases and the cell surface: novel roles in normal and malignant cell physiology. *Adv. Cancer Res.*, *78*: 103–157, 2000.
31. Koolwijk, P., van Erck, M. G., de Vree, W. J., Vermeer, M. A., Weich, H. A., Hanemaaijer, R., and van Hinsbergh, V. W. Cooperative effect of TNF $\alpha$ , bFGF, and VEGF on the formation of tubular structures of human microvascular endothelial cells in a fibrin matrix. Role of urokinase activity. *J. Cell Biol.*, *132*: 1177–1188, 1996.
32. Yasunaga, C., Nakashima, Y., and Sueishi, K. A role of fibrinolytic activity in angiogenesis. Quantitative assay using *in vitro* method. *Lab. Investig.*, *61*: 698–704, 1989.
33. Planus, E., Barlovatz-Meimon, G., Rogers, R. A., Bonavaud, S., Ingber, D. E., and Wang, N. Binding of urokinase to plasminogen activator inhibitor type-1 mediates cell adhesion and spreading. *J. Cell Sci.*, *110*: 1091–1098, 1997.
34. Deng, G., Curriden, S. A., Wang, S., Rosenberg, S., and Loskutoff, D. J. Is plasminogen activator inhibitor-1 the molecular switch that governs urokinase receptor-mediated cell adhesion and release? *J. Cell Biol.*, *134*: 1563–1571, 1996.
35. Yebra, M., Parry, G. C. N., Stromblad, S., Mackman, N., Rosenberg, S., Mueller, B. M., and Cheresch, D. A. Requirement of receptor-bound urokinase-type plasminogen activator for integrin  $\alpha$ v $\beta$ 5-directed cell migration. *J. Biol. Chem.*, *271*: 29393–29399, 1996.
36. Chicurel, M. E., Singer, R. H., Meyer, C. J., and Ingber, D. E. Integrin binding and mechanical tension induce movement of mRNA and ribosomes to focal adhesions. *Nature (Lond.)*, *392*: 730–733, 1998.
37. Stack, M. S., Gately, S., Bafetti, L. M., Enghild, J. J., and Soff, G. A. Angiostatin inhibits endothelial and melanoma cellular invasion by blocking matrix-enhanced plasminogen activation. *Biochem. J.*, *340*: 77–84, 1999.
38. Yokoyama, Y., Dhanabal, M., Griffioen, A. W., Sukhatme, V. P., and Ramakrishnan, S. Synergy between angiostatin and endostatin: inhibition of ovarian cancer growth. *Cancer Res.*, *60*: 2190–2196, 2000.
39. Lehti, K., Valtanen, H., Wickström, S., Lohi, J., and Keski-Oja, J. Regulation of membrane-type-1 matrix metalloproteinase activity by its cytoplasmic domain. *J. Biol. Chem.*, *275*: 15006–15013, 2000.
40. Woods, A., and Couchman, J. R. Syndecans: synergistic activators of cell adhesion. *Trends Cell Biol.*, *8*: 189–192, 1998.
41. Sasaki, T., Larsson, H., Kreuger, J., Salmivirta, M., Claesson-Welsh, L., Lindahl, U., Hohenester, E., and Timpl, R. Structural basis and potential role of heparin/heparin sulfate binding to the angiogenesis inhibitor endostatin. *EMBO J.*, *18*: 6240–6248, 1999.